Received: 3 August 2021 | Revised: 3 November 2021 | Accepted: 14 December 2021

DOI: 10.1002/mmce.23050

ORIGINAL ARTICLE

INTERNATIONAL JOURNAL OF RF AND MICROWAVE COMPUTER-AIDED ENGINEERING WILEY

Low profile and miniaturized dual-band antenna based on graphene assembled film for wearable applications

Chen Wang | **Rongguo Song** | **Shaoqiu Jiang** | **Zelong Hu** | **Daping He**

Hubei Engineering Research Center of RF-Microwave Technology and Application, Wuhan University of Technology, Wuhan, China

Correspondence
Rongguo Song and Daping He, Hubei Engineering Research Center of RF-Microwave Technology and Application, Wuhan University of Technology, Wuhan 430070, China.
Email: rongguo_song@whut.edu.cn (R. S.) and hedaping@whut.edu.cn (D. H.)

Funding information
National Natural Science Foundation of China, Grant/Award Number: 51701146. Fundamental Research Funds for the Central Universities, Grant/Award Number: 206814004. National innovation and entrepreneurship training program for college students, Grant/Award Number: 202110497052.

Abstract

Wearable electronic devices are the basic components of wireless human body local area network. Due to their close contact with the human body, it is necessary to improve the flexibility and isolation of the antenna to maintain high signal transmission performance. In this paper, a flexible wearable antenna based on highly conductive graphene assembled film (GAF) and polydimethylsiloxane dielectric material is proposed. The planar combination of the powerful novel materials and supple polymer maximizes the flexibility and chemical stability of the antenna. In addition, the coplanar waveguide feeding and artificial magnetic conductor (AMC) structure enhance the efficiency and isolation with an easier preparation process. In the wearing measurement, the GAF antenna operates at 3.5 GHz for 5G communication frequency band and 5.8 GHz for ISM (Industrial, Scientific, Medical) frequency band. The GAF antenna has a minimizes SAR level, which in accordance with IEEE C95.1 International standard, by taking up a small space with $50.5 \times 48.5 \times 2.08$ mm^3. Furthermore, the GAF antenna has good radiation performance both under several different bending conditions and human body conditions.

KEYWORDS

graphene antenna, low profile, metamaterials, miniaturized, wearable antenna

1 | INTRODUCTION

The arrival of the fifth generation of mobile communication systems (5G) means that the performance of wireless electronic devices will be stronger, the delay will be lower, and the connection will be more stable. The wireless body area network (WBAN), as an important branch of 5G, is also the key to realize the interconnection between the human body and the device, which will surely lead to an explosive progress in scientific research. Regardless of the civilian or military fields, in medical testing equipment, wireless VR, AR interaction, wearable communication equipment and other networked systems that require the human body to receive or send signals, wearable antennas that can bend conformally or even bend flexibly at high frequencies Are the key issues of research. Compared with traditional antennas, more requirements are put forward for new wearable antennas to meet its various functional requirements in the wearable field. For example: To solve the bending limitations of traditional antennas in various application scenarios caused by metal fatigue; Work out the antenna life issues facing long-term wearing conditions (such as corrosion resistance and waterproof performance); Passed three additional indicators: human body condition test, bending condition test, and absorption ratio test (SAR).[1] In recent years, there has been a lot of research in the field of wearable antennas, and the ideas for solving problems

Chen Wang and Rongguo Song contributed equally to this work.

are concentrated in two directions: one is the flexibility of conductive and dielectric materials, especially the former, and the other is the design innovation of new antenna structures.

In terms of new flexible materials: just as people imagine for wearable antennas, directly endowing conductivity to textiles to achieve high-efficiency antenna radiation is the most reasonable method. The most direct is to prepare a metal thread and weave it with textiles.[2,3] This method can effectively control the conductivity of the textile by adjusting the density of the metal wire, but the preparation process is too troublesome and poor in repeatability. There are also researches electroplating copper or tin on nylon.[4] Although this material has a simpler and more precise preparation method, it still inevitable that large-scale metal oxidation. In order to ensure the service life of the antenna, additional isolation must be done.[5] There are also works that spray or print conductive inks on dielectric materials.[4,6] However, this method can only achieve mass production at the expense of accuracy, and it is difficult to ensure the accuracy of each antenna at the millimeter wave scale. In short, metal is not an ideal material for wearable devices, and current artificial conductive materials cannot become a mainstream solution due to the above-mentioned problems. Graphene, a unique and outstanding two-dimensional carbon-based material, has been well experimentally verified for its flexibility, high strength, water resistance, corrosion resistance, electrical and thermal conductivity,[7–13] which are common rigid requirements for wearable antennas (conformal body bending; clothing folds bending; long-time wearing; sweat infiltration). Moreover, the increasingly abundant graphene raw materials and more mature graphene processing, antenna printing, laser engraving molding and other technologies, make the price and complexity of graphene antenna preparation compared to metal antennas is cheaper and simpler. Therefore, graphene is expected to make up for the defects of existing artificial materials, as an important flexible conductive material in the wearable field.

Moreover, in terms of the optimization and innovation of the new antenna structure, there are some researches to directly reduce the back radiation of the antenna itself, but this often only enhances the isolation between the human body and the antenna, and cannot take into account the bending strength,[14–19] even if it is made of flexible materials.[20] From this point of view, it is extremely challenging to design a single antenna with high body isolation and strong bending resistance. A periodic artificial material similar to phononic crystals—metamaterials has been proposed. It can precisely control the reflection and refraction of waves at the same time through sophisticated structural design, which is in line with our requirements for reducing human body radiation and increasing main lobe gain. The following are several metamaterial structures commonly used in the field of radio frequency and microwave: Electromagnetic band gap structure (EBG);[4,21] artificial magnetic conductor (AMC);[20,22–24] and other structures with similar functions.[25,26] Purposefully use of the metamaterial structure, the classic antenna can also realize wearable functions.

In this work, we investigate a high-performance graphene assembled film (GAF) as a conductive material, which uses graphene oxide as a raw material and is prepared by high-temperature annealing and high-pressure processing. The surface resistance of the GAF is 36 mΩ/sq, and the conductivity is 1.11×10^6 S/m with the thickness is 25 μm. The designed antenna reflecting surface adopts the AMC structure, which enhances the human body isolation, main lobe gain, and supplements partial circular polarization characteristics at the 5G-communication and ISM frequency bands. At 3.5 and 5.8 GHz, the GAF antenna has relative bandwidth of 7% and 12%, high gain of 9.35 and 10.03 dBi, low SAR level under the average 1 g organization 0.187 and 0.43 W/kg (significantly less than the international standard 1.6 W/kg), respectively. In addition, the GAF antenna has good performance stability in bending state and wearing human body. Flexible and dual-band GAF wearable antenna proposed in this work will be of great significance for WBAN, flexible electronics, and wearable devices.

2 | PRINCIPLE AND CONFIGURATION

In this section, we will elaborate on the detailed structure and the fabrication process of our antenna (as shown in Figure 1 and Table. 1) and its foremost operating principle (as shown in Figure 2), The specific explanation is divided into the following three parts:

2.1 | AMC design

The reflection rule of AMC comes from its surface impedance which changes with the change of resonance frequency, the equivalent circuit is shown in Figure 2A, due to the substrate completely separates the reflective surface and the ground structure, it forms an LC circuit as a whole. When the incident electromagnetic waves contact the AMC surface, it forms a high-impedance surface at the designed frequency band (determined by the values of L and C), which reflects electromagnetic waves with the same amplitude, while waves in other frequency bands penetrate the substrate and are absorbed by the

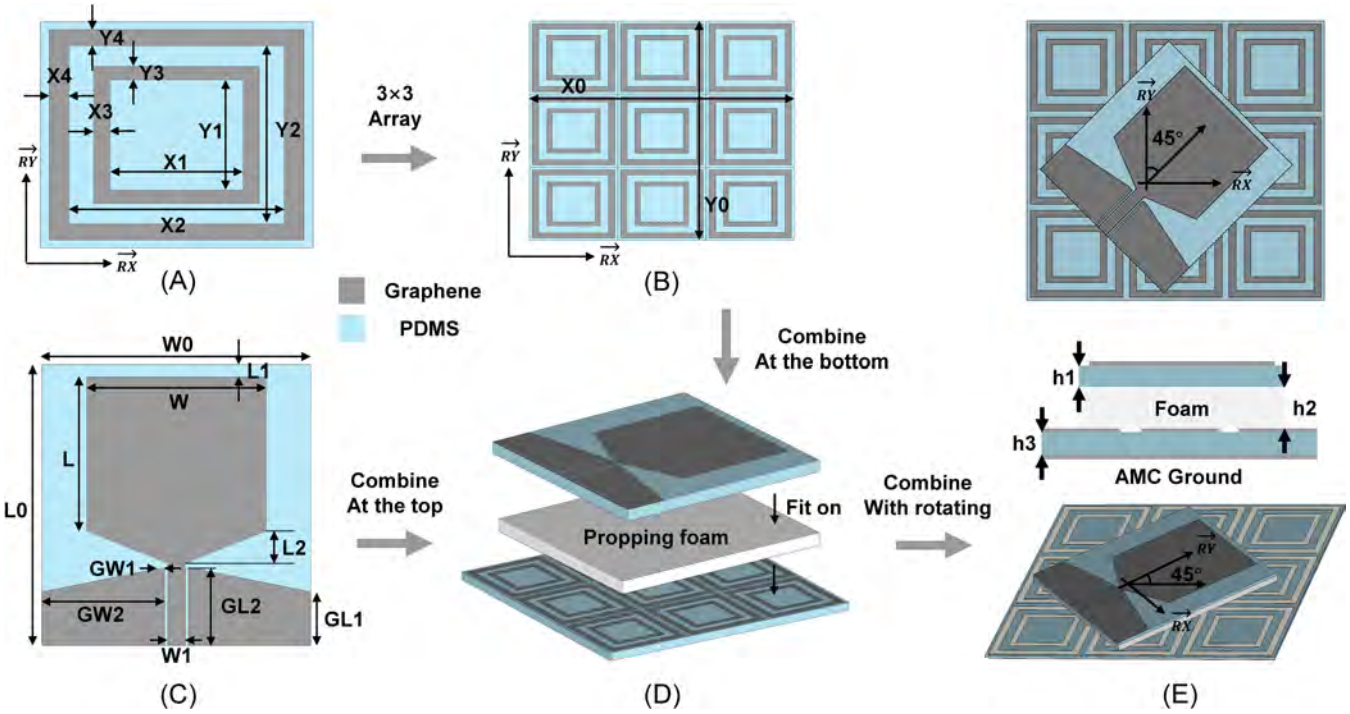

FIGURE 1 (A) AMC cycle unit, (B) top view of AMC overall structure with 3 × 3 Array, (C) UWB antenna with CPW design, (D) schematic diagram of the assembly process of the antenna, (E) top view, front view, and oblique view of the antenna

TABLE 1 Antenna structure parameters

Parameter	Value (mm)	Parameter	Value (mm)	Parameter	Value (mm)	Parameter	Value (mm)
X0	50.5	Y1	48.5	W	20	L	17.2
X1	8.2	Y2	7.88	W0	30	L0	31
X2	13.26	Y3	12.74	W1	2	L1	9.2
X3	1.02	Y4	0.98	GW1	0.8	GL1	6
X4	1.21	Y5	1.17	GW2	13.7	GL2	8.6
h1	0.5	h2	1	h3	0.5	L2	3.6

ground. The detailed process is also shown in Figure 2A, when there is a wave source radiating to the forward and backward at the same time, correspondingly produce the direct radiation wave E-direct (E^d) and the reflected wave E-reflect (E^r) (which after the phase transformation by the AMC reflector), which coupling interference to each other, finally get the modulated electromagnetic wave E-modulated (E^m) required by our design. So, there are many ways to design the surface impedance of AMC, such as the simplest square array,[20,27] I-shaped array,[25] or more complex structures,[22,24] despite all distinct changes, the periodicity is indispensable. Obviously, when we consider a flat rectangular array, if different impedance designs are used in the length and width, it will bring different phase changes to the reflected wave. We use simulation to fully demonstrate this phenomenon in Figure 2B. The two basic modes of electromagnetic waves, TE and TM, are respectively coupled with the long side and short side of the AMC. Corresponding to this article, Reflect-X (*RX*) and Reflect-Y (*RY*) is used instead. Just focus on one side, the lower frequency band corresponds to a lager period unit, while higher frequency band corresponds to a smaller period unit. Using the above-mentioned special properties, we can place the radiation source at an offset of 45° above the reflecting surface (as shown in Figure 1E). Then the two components, RX and RY will obtain the equal reflected amplitude at the same time. Same amplitude coordinates different phase, we can achieve amounts of useful features, including circular polarization.[27,28] Furthermore, it can be explained from the perspective of mathematical formulas through the analysis of the electric field. The

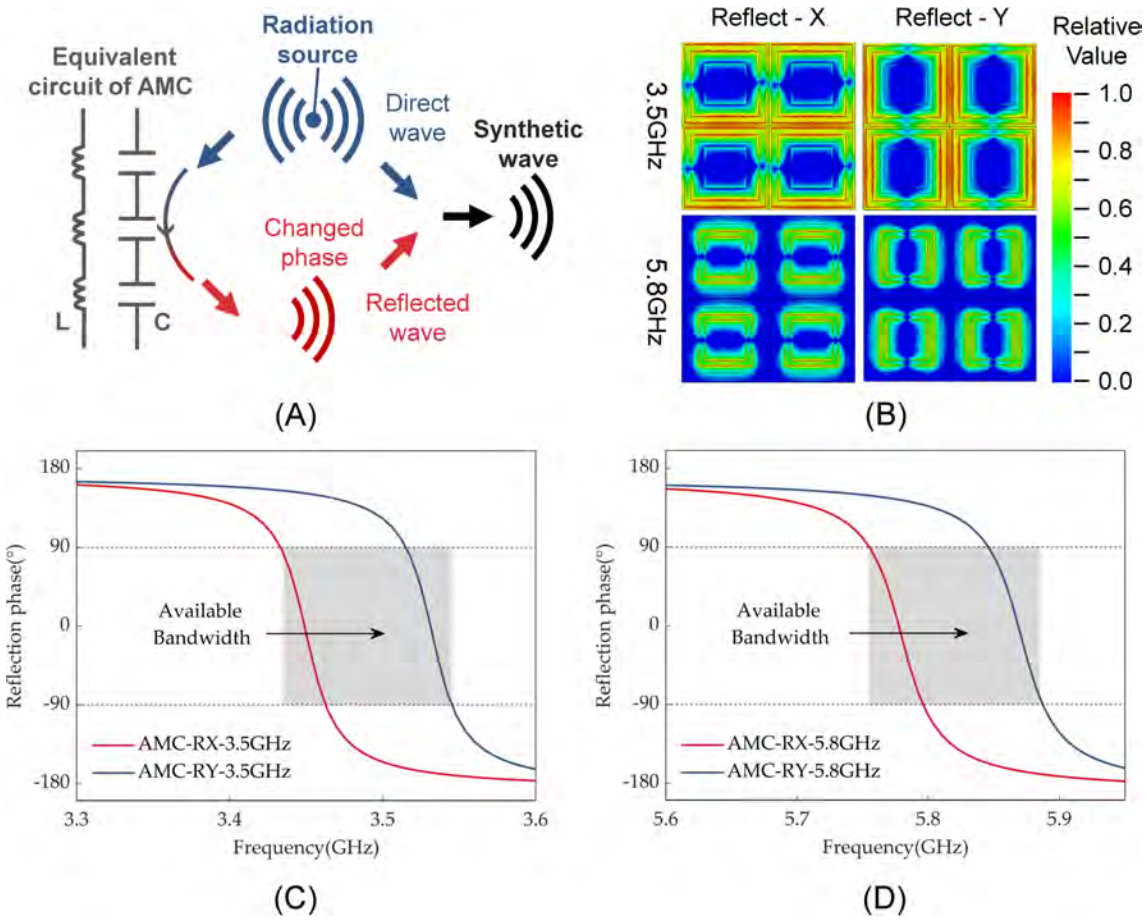

FIGURE 2 (A) Electromagnetic modulation principle of AMC, (B) simulation of AMC modulation principle respectively in direction (Rx and Ry) and frequency, (C) simulation of AMC reflection phase at 3.5 GHz, (D) simulation of AMC reflection phase at 5.8 GHz

following quotes the final formula in the Reference28, which uses a 45° dipole placed above the rectangular periodic reflection structure:

$$\begin{aligned} \vec{E}^{m} &= \vec{E}^{d} + \vec{E}^{r} \\ \vec{E}^{d} &= \frac{E_0}{2}\left(\hat{x}\cdot e^{-jkz} + \hat{y}\cdot e^{-jkz}\right) \\ \vec{E}^{r} &= \frac{E_0}{2}\left(\hat{x}\cdot e^{-jkz-2jkd+j\theta_x} + \hat{y}\cdot e^{-jkz-2jkd+j\theta_y}\right) \end{aligned} \tag{1}$$

where j is the imaginary unit, z is the length variable in the Z direction, k is the wave number, d is the distance between the antenna and the AMC, θx and θy are the reflection phases of RX and RY. The amplitudes in the X and Y directions are both half of the total electric field E0, which perfectly describes the reason for the 45° placement.

If $\theta x = \theta y = 0°$, the reflecting surface constitutes PMC, and the total electric field becomes:

$$\vec{E}^{m} = E_0 e^{-jkz}(\hat{x}+\hat{y}) \tag{2}$$

This method chosen by the majority AMC researches,[20,22–24] whose reflective surface usually adopts a square periodic structure, so that the reflect phase in the X and Y directions is equal. In this way, the gain of a single antenna can be theoretical double.

If $\theta x = 90°$ and $\theta y = -90°$, the reflecting surface can form a right-handed circular polarization, and the total electric field becomes:

$$\vec{E} = \frac{E_0}{2} e^{-jkz}[(\hat{x}+\hat{y}) + j(\hat{x}-\hat{y})] \tag{3}$$

Therefore, in this paper, the AMC cycle unit is designed to be rectangular with different lengths and widths (as shown in Figure 1A), then the unit is periodically arranged into a 3×3 array (as shown in Figure 1B). The rectangular outer ring is coupled with electromagnetic waves at 3.5 GHz, while the inner ring is coupled at 5.8 GHz. Thus, the RX phase change equals −90° and RY equals 90°. The simulation results are shown in Figure 2C and Figure 2D. Since the antenna does not generate ideal vertical incidence and

AMC is also not the overall structure involved in reflection, the bandwidth of AMC can be defined as the shaded part in the Figure 2C,D. The given AMC data has been adjusted after simulating with the antenna to satisfy the right-hand circular polarization (formula (3)).

2.2 | Antenna design

Classic single-frequency patch antennas, such as in-set waveguide microstrip antenna, is essentially equivalent to a dipole composed of a RLC circuit. After bending the radiating element, the resonant length is stretched and the capacitance in the circuit is reduced while the inductance is almost unchanged.[6] The result is that the working frequency is easily shifted to low frequency, which greatly affects the normal operation of the antenna. So, when we implement dual-band antenna in this article, the coplanar waveguide (CPW) design is used (as shown in Figure 1C) to realize the ultra-wideband (UWB) mode. Now, even under the same bending conditions, the bandwidth of antenna changes very little and does not influence the working frequency band. This method greatly improves the robustness of the antenna under distinct wearing conditions and also enhances the radiation efficiency.

2.3 | Overall structure

In summary, the AMC and the antenna are assembled together at a relative angle of 45° (as shown in Figure 1D). In addition, what needs to be emphasized is support layer. A lot of work has introduced new structures for antennas, such as metamaterials, usually using foam as a propping.[20,22,23] This is because the ideal foam material ($\mathcal{E}r = 1$) has little effect on electromagnetic radiation (in formula (1), z is much larger than d), but it still affects the mechanical properties to varying degrees under different thicknesses: when the thickness is small, due to the loose structure, it can flexibly transform under external force, which brings more flexible and variable application performance during wearing;[29] however, when the thickness is too large, the bending angle of the antenna will be strictly limited due to the increase of stress. Therefore, after many experiment attempts, in this article, we decided to use 1 mm thick foam to get the best overall antenna performance. The comprehensive antenna structure view is finally obtained as shown in Figure 1E, and all structure data are listed in Table. 1.

TABLE 2 Comparing the performance of copper and grapheme

Materials	Poisson's ratio	180° Cyclic bending
Copper	0.34	23 times cracked
GAF	−0.26	2000 times no change

3 | FABRICATION AND MEASUREMENT

3.1 | Graphene assemble film

The high-performance GAF used in this paper adopts graphene oxide as the precursor, annealed and carbonized at 1300°C for 2 h, graphitized at 2850°C in an Ar atmosphere for 1 h, finally compressed at 200 MPa to prepare the film. The surface resistivity is 36 mΩ/sq, Therefore, the conductivity of 25 μm GAF used in this article can reach 1.11×10^6 S/m which is far beyond textile conductive materials.[30,31] Furthermore, the GAF has tremendous mechanical properties[32] and passed the 180° large-angle cyclic bending pressure test.[8,11,33] The results are shown in Table. 2. Compared with copper. It is obvious that GAF win the contrast. This means that graphene can be soaked in sweat for a long time without affecting application function, and the flexible bending ability has an extreme high upper limit, which forcefully proves the superiority of GAF.

3.2 | Antenna

We use laser engraving to process and shape the GAF, then attach a viscous spray ($\mathcal{E}_r = 1$) on the surface, tear off the section other than the required high-precision structure, and paste it on the prepared PDMS. The digital photo of UWB antenna prepared by this method and its scattering coefficient are shown in Figure 3A. It reveals that the part of the bandwidth less than −10 dB ranges from 3.32 to 8.19 GHz, covering 4.87 GHz which means the relative bandwidth of 84.6%. On the other hand, the preparation of AMC remains the same method, superadd the foam structure to prop. The overall structure without configuring AMC ground (to help readers more intuitively distinguish the AMC structure) and scattering coefficient as shown in Figure 3B. There are bandwidths of 3.3-3.54 GHz and 5.52-6.16 GHz respectively at 3.5 and 5.8 GHz while the lowest return loss can reach −22 and −28 dB. The relative measurement of pattern as shown in Figure 4A,B. From the perspective of radiation density, it can be seen that both low frequency and high frequency are weakened in the minor lobe, but low

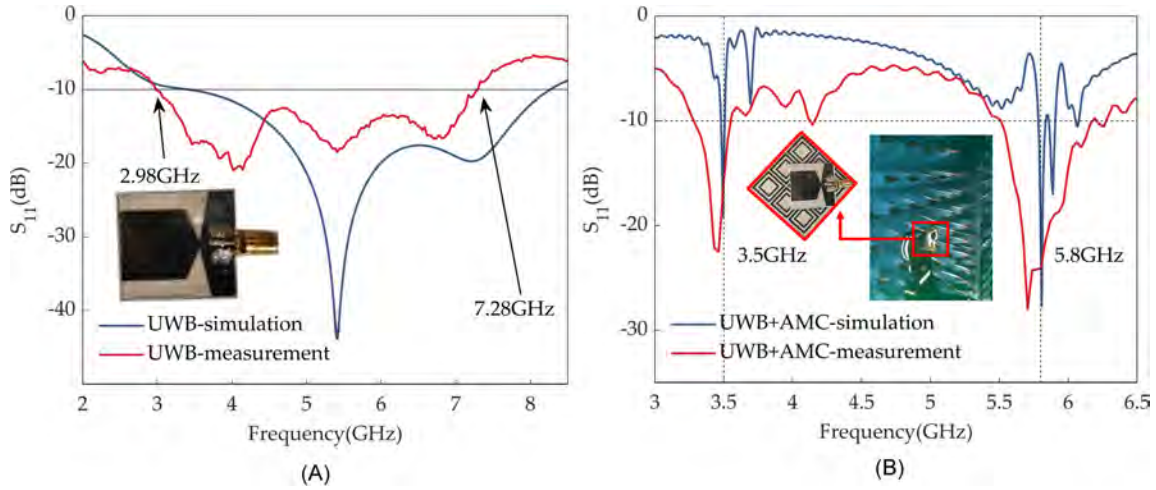

FIGURE 3 (A) UWB antenna digital photo and its simulated and measured reflection coefficient, (B) digital photo of the top view of the overall antenna (AMC without ground in order to display the structure more clearly) and its simulated and measured reflection coefficient

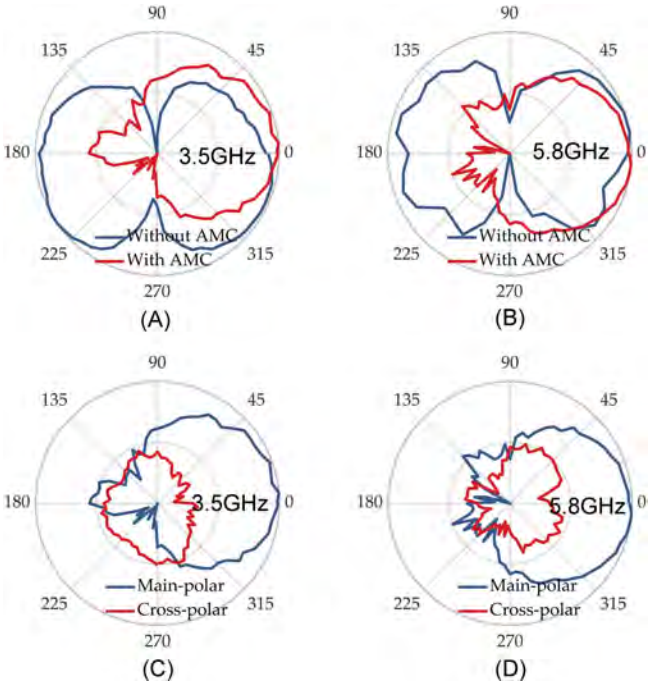

FIGURE 4 The comparative relative measurement results of antenna: (A) Directional pattern with and without AMC at 3.5 GHz, (B) directional pattern with and without AMC at 5.8 GHz, (C) main and cross polarization pattern of overall antenna at 3.5 GHz, (D) main and cross polarization pattern of overall antenna at 5.8 GHz

frequency is not quite effective, it is because the size of miniaturized AMC is appropriate for 5.8 GHz. But at 3.5 GHz, a small number of waves pass through along the AMC surface, transmit without reflection. Thus, forming the peculiar minor lobe phenomenon shown in Figure 4A. Nevertheless, this part of the transmission has little effect on the human body and does not affect the overall isolation between the antenna and the human body. The specific reasons will be explained in detail in the SAR test. The Figure 4C,D show the main and cross polarization pattern, which prove the anti-interference ability of the antenna with right-hand circular polarization. In addition, we show the axial ratio simulation of the antenna in Figure 5A. Less than 3 dB is regarded as the bandwidth range of circular polarization, so high frequency performance is better than low frequency, but all have completed the design expectation of circular polarization. At the same time, the measured gain of the antenna is shown in Figure 5B. The maximum value fits the antenna's forward radiation (angle = 0°), and reach up to 9.35 and 10.03 dBi respectively at 3.5 and 5.8 GHz. By and large, the miniaturized wearable antenna has realized a substantial enhancement.

4 | WEARING PERFORMANCE

4.1 | Bending and on-body condition

As mentioned in the introduction, antennas used in the wearable field must undergo three additional tests, respectively are bending test, on-body test and SAR test. This section will implement a comprehensive measurement of above three aspects: In this article, we adopt cylindrical foams ($\mathcal{E}_r = 1$) with different diameters to realize the different degree of bending to simulate diverse application scenario as shown in Figure 6A. They are 2R = 55 mm corresponding to the shape of the arm while 2R = 70 mm corresponding to the shape of the thigh and 2R = 95 mm corresponding to the shape of the chest or back. In Figure 6B, we roughly show the flexibility and compatibility of the GAF and PDMS under bending and

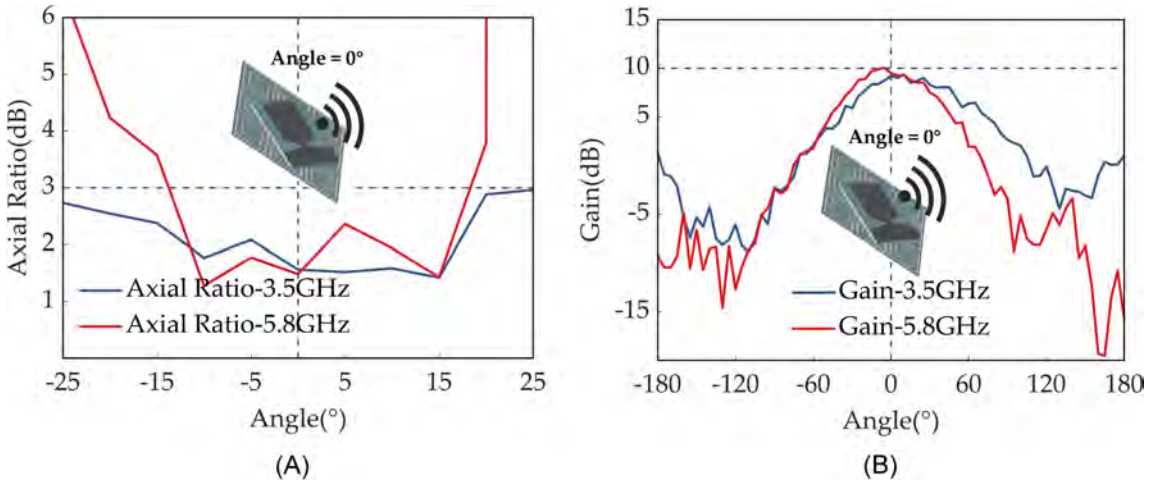

FIGURE 5 Measurement results of the antenna with AMC assembled: (A) The measurement axial ratio of overall antenna, (B) the measurement gain of overall antenna

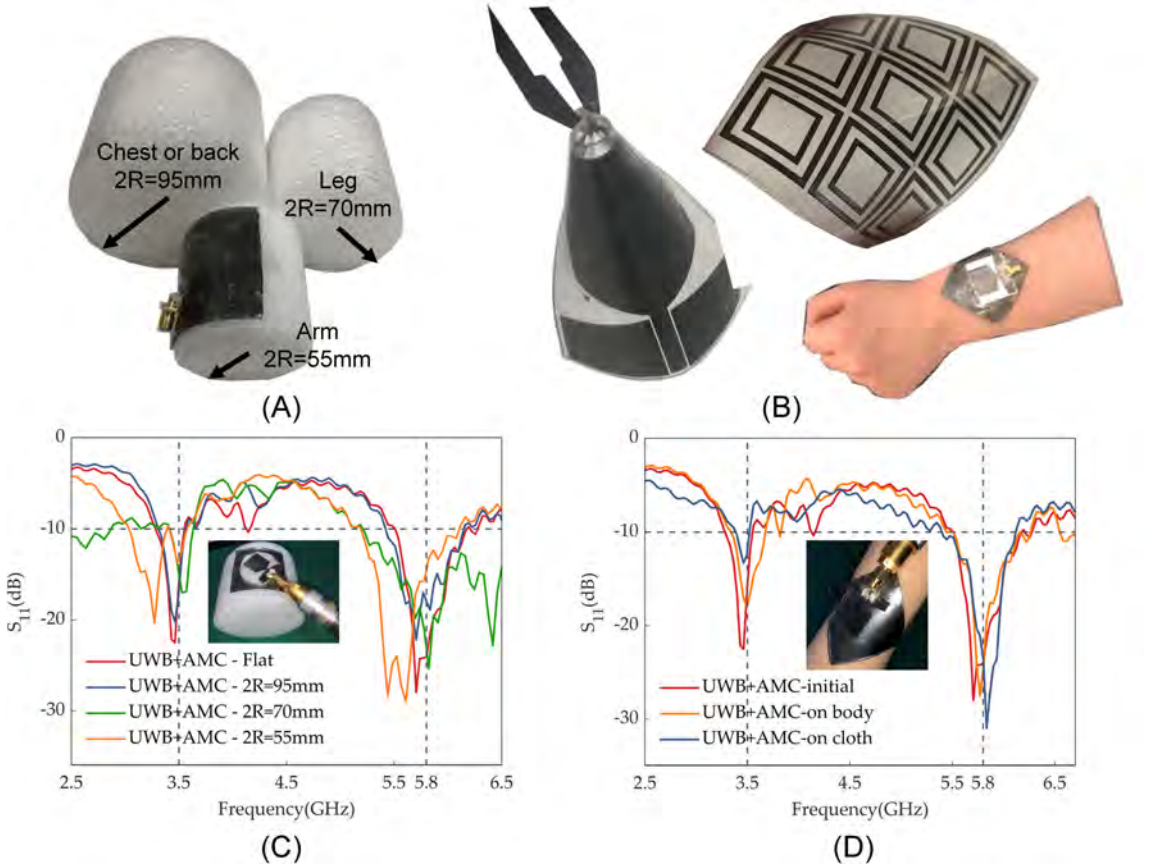

FIGURE 6 (A) Digital photo of the foam used in the scene simulation, (B) flexibility and compatibility display of different structures, (C) measurement of reflection coefficient at different bending condition, (D) measurement of reflection coefficient at different wearing condition

on-body condition. The performance of the scattering coefficient is shown in Figure 6C. In the case of a slight bending: the low-frequency part has a small attenuation while the high frequency part does not change too much; In the case of an intense bending, there is a subtle frequency deviation. Part of the reason for the above phenomenon is when the deflection is too large, the foam deforms unevenly. Resulting in the distance between the

antenna and the AMC varies irregularly. Another part of the reason is AMC optimum size problem what we mentioned earlier, a small number of low frequency waves pass through along the AMC surface, transmit without reflection. Nonetheless, the antenna can still work normally at 3.5 and 5.8 GHz, holistic final performance is in line with the original design expectations. The above results are for reference only in order to illustrate the flexibility of the antenna and its robustness to bending. However, as far as the human body is concerned, it is composed of a variety of tissues whose dielectric constant and density distribution are complicated, and its influence on electromagnetic fields is deserved intricate. In the Reference15, a targeted analysis was made. The body, head, and clothing, respectively weakened the radiation performance of 19.2, 13.0, and 1.7 dB. However, since the outline of head belongs to non-Euclidean geometry, the bending process is more complicated and the results are unstable and unrepeatable. Therefore, we precisely executed the tests on arms and clothes as shown in Figure 6D. The results reveal that in the low frequency part, there is always an attenuation. This is consistent with the bending test results. Long wave is not completely reflected by the AMC, but are transmitted from the edge of the structure to below the AMC. In extreme cases, this phenomenon will be exacerbated and eventually absorbed by the human body or scattered into the air. The high frequency part has also performed very well because of the optimum size of AMC, maintaining a relative bandwidth of 12%. In summary, the antenna has good human body robustness which accomplish outstanding performance as expected under harsh conditions of wearing.

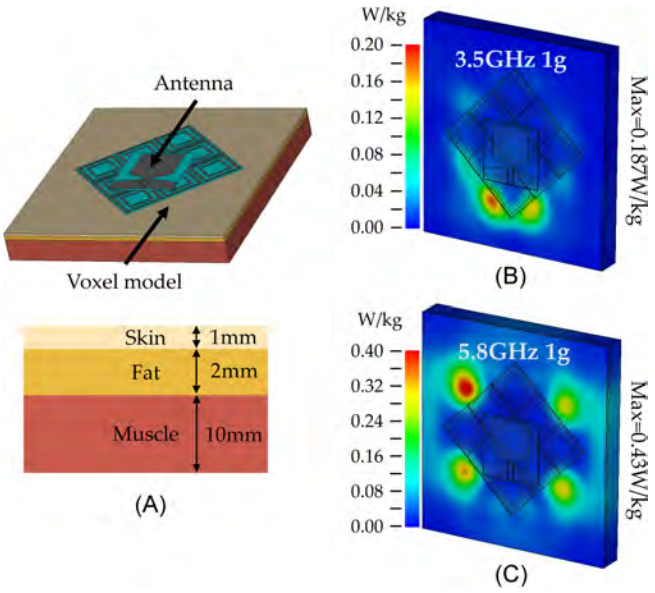

FIGURE 7 (A) The simulation diagram of integral antenna structure and section height of each part, (B) SAR result at 3.5 GHz, (C) SAR result at 5.8 GHz

TABLE 3 Parameters of human tissues

Voxel data	Ɛr	σ [S/m]	P [kg/m3]
Skin	38.0067	1.46407	1100
Fat	6.07388	0.03629	1100
Muscle	54.4176	1.88201	1040

4.2 | SAR simulation

As a wearable antenna, it faces the possibility of long-term wearing, so we have to minimize its possible detrimental impact on human. The SAR parameter is an essential criterion for measuring the absorption of antenna radiation by

TABLE 4 Comparison of some significant data in wearable antenna field

References	Structure	Materials	Frequency (GHz)	Profile (mm)	Size ($\lambda_0 \times \lambda_0$)	Gain (dBi)	Practicability
17	HMSIW	Metal	5.2/5.8	1.57	0.67 × 0.67	3.31/4.16	Non-flexible
18	HMSIW	Metal	8–12	0.787	0.67 × 0.67	5.3/4.3	Non-flexible
19	SIW	Metal	8.6/13.4	1.57	0.74 × 0.86	5.1/6.3	Non-flexible
20	AMC	Metal	5.7–11.0	5.74	0.87 × 0.87	8	Non-flexible
22	AMC	Metal	2.45	9.5	0.41 × 0.41	−2.5	Non-flexible
23	AMC	Metal	3.5/5.8	4.62	1.00 × 1.00	9.373/6.634	Non-flexible
25	EBG	Metal	2.36–2.4	4	0.49 × 0.34	6.2	Non-flexible
4	EBG	Textile	2.45/5.8	3.3	0.98 × 0.98	—	Flexible
21	EBG	Textile	2.45	4	0.66 × 0.66	7.3	Flexible
27	AMC	Graphene	5.8	2.57	0.87 × 0.75	6.1	Flexible
This work	AMC	GAF	3.5/5.8	2.08	0.58 × 0.56	9.35/10.03	Flexible

our human body. Ac-cording to IEEE C95.1, the maximum absorption value of the human body must be less than 1.6 W/kg under the electromagnetic wave radiation of 1 g of human tissue for 6 minutes on average. In this paper, we constructed a 50 × 50 × 13 mm rectangular parallelepiped structure in the CST to simulate human tissue which is composed of skin, fat, and muscle. Its configuration and thickness are both shown in Figure 7A. The dielectric constant, conductivity and density data used to calculate SAR are given in Table. 3. The final result of heat absorption distribution map shows in the Figure 7B,C, the maximum SAR level at 3.5 and 5.8 GHz, respectively are 0.187 and 0.43 W/kg, both are less than 1.6 W/kg, which complies with international safety standards. In general, although the modulation efficiency of the miniaturized AMC for electromagnetic waves at low frequencies is not as expected as that for high frequencies, both the radiation efficiency in the forward direction and the impact on the human body in the back direction (from the perspective of consequentialism) are both within the scope of the design requirements, the process proposed in this article can be a qualified and efficient method for preparing miniaturized wearable antennas.

5 | DISUSSION

The above exhibits all the experimental data in this work, which focus on the two major indicators of wearing conditions: isolation and flexibility. The results prove that it achieves excellent performance under on-human and conformal/bending conditions while a miniaturized antenna scale is limited. This work validates an improved performance among most wearable antenna researches with exploiting metasurface as a reflector. Consequently, in Table. 4, we list several consistent investigations which operate EBG and AMC structure, and compared some significant data like antenna's size, gain and wearing performance. Compared with previous wearable antennas with metamaterial structures, an important improvement of efficiency in our work is that our GAF conductivity has exceeded 10^6, compared to textiles and printing inks with only 10^4, we have a lower loss so that the antenna will have an outstanding performance in the centimeter wave and even the millimeter wave band. Compared with the traditional dual-band antenna, our double-layer structure scatters electromagnetic waves to cause secondary propagation, which must have energy loss, however, we can analyze the measurement gain that we have average enhancement about twice times. It means that less energy is lost from the side lobes, which is more obvious at low frequency shown in Figure 4A,B. The listed data in the table also reveals that the conventional wearable antenna researches comparatively focus on isolation, that is, the performance of the antenna under on-human condition and SAR level, but ignore the bending/conformal conditions. One of the crucial reasons is that the metal fatigue is inevitable so that greatly compromises the performance of the antenna. The second is the thickness. An excessively thick antenna profile will awfully increase the difficulty of bending and limit the flexibility and elasticity. Therefore, in the future, in order to make up for the defects of metals and satisfy urgently need for suppleness and conductivity. Graphene, the impressive conductive materials, will have a non-negligible potential in the application of wearable antennas, which deserves our more considerable and targeted research and more significant and substantial innovation.

6 | CONCLUSIONS

In conclusion, a miniaturized, low-profile dual-band wearable antenna based on high performances GAF is presented. The GAF antenna has good return loss and radiation capabilities at 5G communication band (3.5 GHz) and ISM band (5.8 GHz). The low profile GAF AMC structure with the size of 50.5 × 48.5 × 2.08 mm^3 simultaneously achieves the minor lobe radiation suppression and main lobe radiation enhance. The SAR values of GAF wearable antenna are under 0.187 and 0.43 W/kg in line with international IEEE standard. In addition, GAF antenna has good radiation ability in bending state and loading human body. Therefore, flexible GAF wearable antenna is a mighty contender in the wireless human body local area network system.

ACKNOWLEDGMENT

This work was supported by the National Natural Science Foundation of China (51701146), the Fundamental Research Funds for the Central Universities (WUT: 206814004) and the National innovation and entrepreneurship training program for college students (202110497052).

DATA AVAILABILITY STATEMENT

The data that supports the findings of this study are available in the supplementary material of this article.

ORCID

Daping He https://orcid.org/0000-0002-0284-4990

REFERENCES

1. El GM, Fernandez-Garcia R, Ahyoud S, Gil I. A review of flexible wearable antenna sensors: design, fabrication methods, and applications. *Materials*. 2020;13(17):3781.
2. Ouyang Y, Chappell WJ. High frequency properties of electrotextiles for wearable antenna applications. *IEEE Trans Antennas Propag*. 2008;56(2):381-389.

3. Roh J-S, Chi Y-S, Lee J-H, Tak Y, Nam S, Kang TJ. Embroidered wearable multiresonant folded dipole antenna for FM reception. *IEEE Antennas Wireless Propag Lett*. 2010;9:803-806.
4. Zhu S, Langley R. Dual-band wearable textile antenna on an EBG substrate. *IEEE Trans Antennas Propag*. 2009;57(4):926-935.
5. Scarpello ML, Kazani I, Hertleer C, Rogier H, Vande GD. Stability and efficiency of screen-printed wearable and washable antennas. *IEEE Antennas Wireless Propag Lett*. 2012;11:838-841.
6. Lin CP, Chang CH, Cheng YT, et al. Development of a flexible SU-8/PDMS-based antenna. *IEEE Antennas Wireless Propag Lett*. 2011;10:1108-1111.
7. Akinwande D, Petrone N, Hone J. Two-dimensional flexible nanoelectronics. *Nat Commun*. 2014;5:5678.
8. Fan C, Wu B, Song R, Zhao Y, Zhang Y, He D. Electromagnetic shielding and multi-beam radiation with high conductivity multilayer graphene film. *Carbon*. 2019;155:506-513.
9. Geim AK, Novoselov KS. The rise of graphene. *Nat Mater*. 2007;6(3):183-191.
10. Song R, Wang Q, Mao B, et al. Flexible graphite films with high conductivity for radio-frequency antennas. *Carbon*. 2018;130:164-169.
11. Wang Z, Li P, Song R, et al. High conductive graphene assembled films with porous micro-structure for freestanding and ultra-low power strain sensors. *Sci Bull*. 2020;65(16):1363-1370.
12. Wang Z, Mao B, Wang Q, et al. Ultrahigh conductive copper/large flake size graphene heterostructure thin-film with remarkable electromagnetic interference shielding effectiveness. *Small*. 2018;14(20):1704332.
13. Lee U, Han Y, Lee S, et al. Time evolution studies on strain and doping of graphene grown on a copper substrate using Raman spectroscopy. *ACS Nano*. 2020;14(1):919-926.
14. Casula GA, Michel A, Nepa P, et al. Robustness of wearable UHF-band PIFAs to human-body proximity. *IEEE Trans Antennas Propag*. 2016;64(5):2050-2055.
15. Mendes C, Peixeiro C. A dual-mode single-band wearable microstrip antenna for body area networks. *IEEE Antennas Wireless Propag Lett*. 2017;16:3055-3058.
16. Agneessens S, Lemey S, Vervust T. Wearable, Small, and robust: the circular quarter-mode textile antenna. *IEEE Antennas Wireless Propag Lett*. 2015;14:1482-1485.
17. Kumar A, Chaturvedi D, Raghavan S. Design and experimental verification of dual-fed, self-diplexed cavity-backed slot antenna using HMSIW technique. *IET Microw Antenna Propag*. 2019;13(3):380-385.
18. Althuwayb AA, Al-Hasan MJ, Kumar A, Chaturvedi D. Design of half-mode substrate integrated cavity inspired dual-band antenna. *Int J RF Microw Comput-Aided Eng*. 2021;31(2):e22520.
19. Kumar A, Saravanakumar M, Raghavan S. Dual-frequency SIW-based cavity-backed antenna. *AEU-Int J Electron C*. 2018;97:195-201.
20. Liu X, Di Y, Liu H, Wu Z, Tentzeris MM. A planar windmill-like broadband antenna equipped with artificial magnetic conductor for off-body communications. *IEEE Antennas Wireless Propag Lett*. 2016;15:64-67.
21. Gao GP, Hu B, Wang SF, Yang C. Wearable circular ring slot antenna with EBG structure for wireless body area network. *IEEE Antennas Wireless Propag Lett*. 2018;17(3):434-437.
22. Agarwal K, Guo YX, Salam B. Wearable AMC backed near-endfire antenna for on-body communications on latex substrate. *IEEE Trans Compon, Packag Manuf Dent Tech*. 2016;6(3):346-358.
23. Atrash ME, Abdalla MA, Elhennawy HM. A wearable dual-band low profile high gain low SAR antenna AMC-backed for WBAN applications. *IEEE Trans Antennas Propag*. 2019;67(10):6378-6388.
24. Genovesi S, Costa F, Fanciulli F, Monorchio A. Wearable inkjet-printed wideband antenna by using miniaturized AMC for sub-GHz applications. *IEEE Antennas Wireless Propag Lett*. 2016;15:1927-1930.
25. Jiang ZH, Brocker DE, Sieber PE, Werner DH. A compact, low-profile metasurface-enabled antenna for wearable medical body-area network devices. *IEEE Trans Antennas Propag*. 2014;62(8):4021-4030.
26. Amiri MA, Balanis C, Birtcher CR. Gain and bandwidth enhancement of a spiral antenna using a circularly symmetric HIS. *IEEE Antennas Wireless Propag Lett*. 2017;16:1080-1083.
27. Zu HR, Wu B, Zhang YH, et al. Circularly polarized wearable antenna with low profile and low specific absorption rate using highly conductive graphene film. *IEEE Antennas Wireless Propag Lett*. 2020;19(12):2354-2358.
28. Fan Y, Rahmat-Samii Y. A low profile single dipole antenna radiating circularly polarized waves. *IEEE Trans Antennas Propag*. 2005;53(9):3083-3086.
29. Hertleer C, Rogier H, Vallozzi L, Van Langenhove L. A textile antenna for off-body communication integrated into protective clothing for firefighters. *IEEE Trans Antennas Propag*. 2009;57(4):919-925.
30. Hamouda Z, Wojkiewicz JL, Pud AA, et al. Dual-band elliptical planar conductive polymer antenna printed on a flexible substrate. *IEEE Trans Antennas Propag*. 2015;63(12):5864-5867.
31. Hamouda Z, Wojkiewicz JL, Pud AA, Kone L, Bergheul S, Lasri T. Magnetodielectric nanocomposite polymer-based dual-band flexible antenna for wearable applications. *IEEE Trans Antennas Propag*. 2018;66(7):3271-3277.
32. Li P, Wang Z, Song R, et al. Customizable fabrication for auxetic graphene assembled macrofilms with high conductivity and flexibility. *Carbon*. 2020;162:545-551.
33. Song R, Zhao X, Wang Z, et al. Sandwiched graphene clad laminate: a binder-free flexible printed circuit board for 5G antenna application. *Adv Eng Mater*. 2020;22(10):2000451.

How to cite this article: Wang C, Song R, Jiang S, Hu Z, He D. Low profile and miniaturized dual-band antenna based on graphene assembled film for wearable applications. *Int J RF Microw Comput Aided Eng*. 2022;32(4):e23050. doi:10.1002/mmce.23050